Test-Analysis Modal Correlation of Rocket Engine Structures in Liquid Hydrogen - Phase II

Andrew M. Brown, Ph.D.[a], Jennifer L. DeLessio[b]

[a] Aerospace Engineer, NASA/Marshall Space Flight Center,
ER41/Propulsion Structural & Dynamic Analysis, Huntsville, AL 35812
[b] Propulsion Systems Analyst, JSEG/ESSCA – NASA/Marshall Space Flight Center,
ER41/Propulsion Structural & Dynamic Analysis, Huntsville, AL 35812

ABSTRACT

Many structures in a launch vehicle operate in liquid hydrogen, from the hydrogen fuel tanks through the ducts and valves and into the turbopumps. Calculating the structural dynamic response of these structures is critical for successful qualification, but accurate knowledge of the natural frequencies is based entirely on numerical or analytical predictions since testing in operating conditions is problematic. A comprehensive test/analysis program has therefore been performed at NASA/MSFC to enable accurate prediction of the modal characteristics of the Space Launch System's (SLS) RS-25 Low Pressure Fuel Turbopump Inducer including the effects of fluid-added mass, mechanical property change at cryogenic temperatures, operation within tight tip clearances, acoustic/structure interaction, and hydroelasticity. The process also has to account for complicated cyclic symmetry mode shapes which can be easily mistuned in test, and geometric, boundary condition, and material modifications between the sub-scale inducer used as a test article and the actual flight component. The first phase of the program, documented previously, focused on testing of a cantilever beam in a number of fluids and temperatures to isolate the effects of fluid-added mass and temperature, while the second phase reported here documents the additional issues associated with the more realistic inducer test article. Preliminary structural dynamic analysis of the flight hardware including variability for the above parameters indicated potential severe resonances, requiring implementation of undesired programmatic constraints, so the improved predictive capability may allow removal of these constraints.

Keywords: Structural Dynamics, Modal Test, Liquid Hydrogen, Model Correlation, Fluid-Structure Interaction

NOMENCLATURE

A_{m1}	added mass for beam-type modes
a	cantilever beam length
b	beam width
{f}	Vector of Natural Frequencies
[Φ]	Modal Matrix
DOF	Degrees of Freedom
DOE	Design of Experiments
E	Young's Modulus
HOC	Higher Order Cavitation
HOSC	Higher Order Surge Cavitation
LDV	Laser Doppler Vibrometer
LH2	Liquid Hydrogen

LOX	Liquid Oxygen
LPFP	Low Pressure Fuel Pump
MAC	Modal Assurance Criterion
ND	Nodal Diameter
RT	Room Temperature
ρ_f	fluid mass density
SLS	Space Launch System
SSME	Space Shuttle Main Engine
ω_f	natural frequency of the beam immersed in fluid
ω_v	natural frequency of the beam in vacuum

INTRODUCTION

Liquid rocket engines are powered by the combustion of two propellants at very high pressure, a fuel and an oxidizer. Frequently, the fuel is liquid hydrogen (LH2). While the pressure can be provided by a very high-strength storage tank, usually this would be weight-prohibitive, so a turbopump or series of turbopumps are required to provide these extremely high pressures. The rotating shafts of these turbopumps are usually driven by a hot gas in the turbine side, and the pumping side consists of either axial inducers, which increase the velocity by conically swept blades on the shaft, or centrifugal impellers, which force the fluid into spinning outward radiating channels; both these actions significantly increase the flow velocity, and high pressures are then obtained by diffusing the flow.

Because of a number of highly-energetic fluid excitation sources at both narrow-band frequency ranges and harmonic frequencies, a structural dynamic analysis is required for all the components in the flow path on both the turbine and pump sides in order to predict possible high dynamic response. Such an analysis is, however, problematic due to a host of complicating factors. First, for liquid hydrogen pumps, the operating temperature is -253°C (-423°F), which has a substantial effect on the Young's Modulus (E) of the metallic materials used for the components, and therefore affects the natural frequencies substantially. Second, the components operate in a liquid, which not only provides the excitation forcing function but also affects both the damping and structural dynamic characteristics (natural frequencies {f} and modes [Φ]) due to virtual mass loading. Making this factor even more complicated is the presence of a wall close to the vibrating structure, which in turbopumps is due to the tight tip-clearance with the housing; a number of studies have validated the intuitive concept that this reduced clearance prevents the fluid from flowing around the object during vibration, thus amplifying the fluid-add-mass and damping effects. Other complicating factors include bubbliness in the fluid due to cavitation from the spinning inducer blades, and compressibility of the fluid, which can cause acoustic modes to interact with the structural modes and change the natural frequencies of both into a combined system mode, and hydroelastic effects, which add flow-velocity dependent effective fluid stiffness and damping terms to the equations of motion.

The difficulty of performing even a basic modal analysis, much less a forced response, therefore, has always been a problem for the design of liquid hydrogen turbopumps, but it became much more of a risk during the design phase of the J-2X engine, from 2006-2012. The frequency range of one of the excitation sources, higher order cavitation (HOC), was predicted to overlap with the oxidizer pump inducer natural frequencies. This motivated an extensive analytical examination, which was forced to incorporate the variability in the structural dynamic characteristics due to the large uncertainties discussed above, and a test program to characterize the environment using high-frequency Kulites to measure dynamic pressure and strain gages mounted on the inducer to measure structural response in a water (not liquid oxygen) rig (see Fig. 1). A great deal of important data was obtained including some information on damping and the mass loading effect of water on the inducer natural frequencies. The most challenging goal of fully anchoring the forcing function and dynamic response was not completed before the J-2X program was cancelled.

The HOC issue existed during operation of the Space Shuttle Main Engine (SSME) and has arisen again during the implementation of the RS-25, which is an updated SSME engine for the core stage of NASA's new Space Launch System. The SSME had shown acceptable margins during extensive testing and operation of over a million seconds,

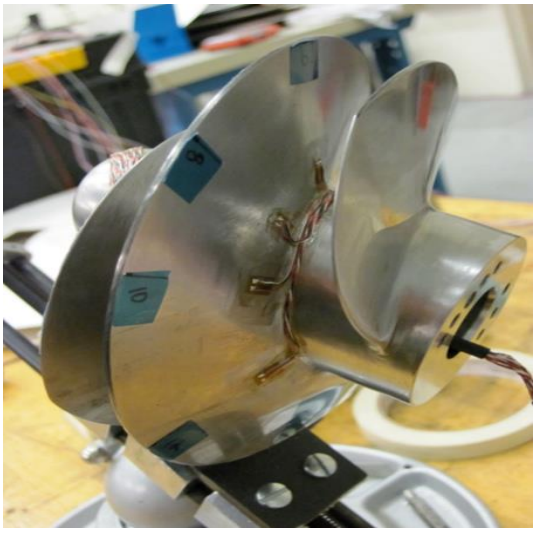

Fig. 1 J2-X Turbopump Inducer (not to scale)

but new operating speeds for the RS-25 with a special circumferentially in-phase case of HOC, called higher order surge cavitation (HOSC), meant those conditions had not been demonstrated by the SSME. An extensive response analysis was performed, but due to the uncertainties discussed above, along with the uncertainties in the forcing function itself, the analysis predicted failure even for SSME operation, which was clearly not accurate. An empirical, non-physics-based damage-fraction analysis was therefore performed based upon one of the tested units, and acceptance criteria stemming from this analysis were imposed upon the inducer and the operation of the turbopump. Some of the resulting speed and operational restrictions are quite undesirable, though, and possibly could be severe if testing shows the magnitude of HOSC are greater than expected.

An integrated test/analysis program was initiated, therefore, both to mitigate some of the restrictions of the criteria and to provide data for a physics-based analysis that would produce believable results. This integrated program includes an updated water flow test, hydroelastic analysis and testing, acoustic modeling, and unique natural frequency testing of the sub-scale stainless-steel inducer in LH2 that was used in the water-flow test. The first phase of this integrated program was completed in 2017 and reported by the authors [1]. That paper detailed the testing of a titanium cantilever beam in water and LH2 and presented the detailed correlation of the numerical model with analytical techniques and the new experimental data. The data proved invaluable to the program in reducing the uncertainties associated with representing the fluid-added mass and the modulus at cryogenic temperatures.

This paper discusses the results and on-going work from the second phase of the integrated test/analysis program. In this phase, first the titanium cantilever plate was re-tested in water and LH2 but this time with plates along its edges to exercise the tip clearance effect. Next, the sub-scale stainless steel inducer was extensively tested with the following series of tests: modal testing in air and water, modal testing in water with a tight clearance, frequency testing in LH2, and testing in a water flow facility which can replicate cavitation and hydroelastic effects (this test will not be discussed in this paper). In concert with the testing, an extensive correlation effort incorporating all the effects from the parameters discussed above was performed for finite/acoustic models of the beam and sub-scale inducer.

LITERATURE SURVEY

Harrison, et al. [2] performed extensive tight-tip clearance testing on a micro-cantilever beam, 1.45 mm X 1.8 mm X 20μm, to examine the effects for sensors. Although much smaller in scale, the effects on natural frequency are the same as for the case discussed in this paper, and two of configurations tested, called “sweep” and “wipe”, match the configurations matched in this paper, which will be discussed in the next section. Key findings from this work are

that the fluid-added mass multiplier is approximately proportional to the inverse of the root of the tip-clearance, but that the value plateaus at close clearances. Green and Sader [3] developed an analytical technique using boundary integrals to calculate the forces on an object when immersed in a fluid with a close rigid boundary vibrating normal to the wall, including the dissipative forces.

This technique is then applied by Xiu and Davis [4] to the case of the object vibrating in a direction parallel to the wall, which is the case of the turbopump inducer blades. The paper presents both the adapted theory and experimental validation for cantilever beams in both the "sweep" and "wiping" configurations previously described by Harrison. Results include detailed curves for both the fluid-added mass (relative to the value without a close boundary) as a function of a non-dimensionalized boundary distance and the fluid-added damping relative to the same parameter. These relationships are extremely valuable and were chosen to serve as a basis for similar testing at MSFC, with the idea of developing numerical modeling techniques using the analytical expressions, and validating these techniques with the experimental results presented by Harrison, Xiu, and at MSFC.

With respect to the effect of compressibility, Davis, Virgin, and Brown [5] examined structural/acoustic interaction extensively; acoustic modes can only exist if compressibility is included in the structural acoustic modal formulations, which had not been done previously to more clearly identify the modes. Motivated by the cracking of an annular structure in an SSME liquid fuel duct, the coupling of structural and acoustic modes was analyzed using numerical and analytical techniques. One of the fundamental results affecting this work was the clear identification of a substantial eigenvalue veering phenomena in a combined structural and acoustic frequency versus nodal diameter plot for LH2 (Fig. 2). For this fluid, if the structural natural frequencies come close in value to the acoustic modal frequencies, the modes will coalesce in a single mode with a different frequency than either of the two media independently.

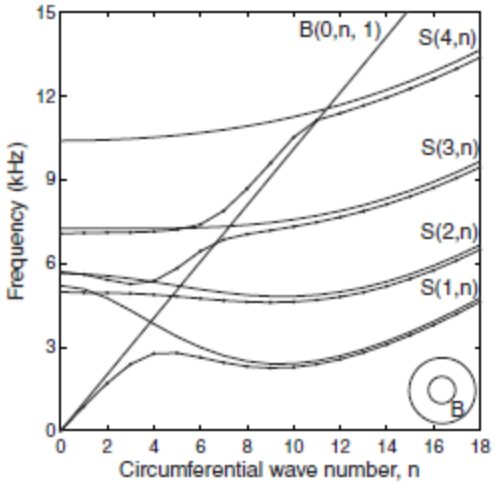

Fig. 2 Structural/Acoustic Nodal Diameter Diagram showing Eigenvalue Veering (from Davis, et al 08)

CANTILEVER BEAM TIGHT TIP-CLEARANCE MODAL TEST AND ANALYSIS

To validate theoretical predictions and optimize meshing techniques to quantify the effect of tight-tip clearance on the fluid-added mass, and in turn the natural frequency, two removable and adjustable side plates were added to the cantilever beam ping-test setup described in Phase I (see Fig. 3). Both one and two-sided configurations were tested. To allow for the greatest possible utility, a number of these configurations were tested in different media (see Table 1), including a liquid Nitrogen test to provide another temperature data point for the Young's Modulus versus Temperature relationship discussed in Phase I.

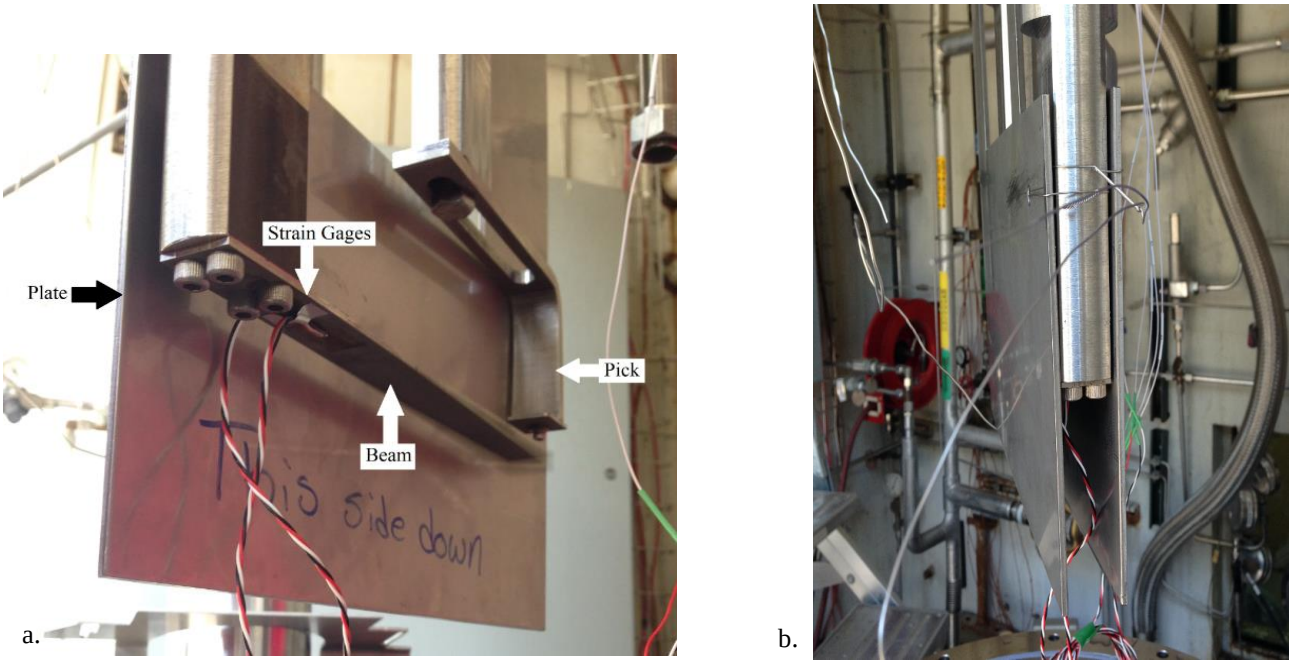

Fig. 3 LH2 Cantilever Beam Ping Test Tight Clearance Setup; a) 1 Sided; b) 2 Sided

Table 1. Cantilever Beam Test Configurations

Configuration Label	Configuration Description
Air-1S	In-air at room temperature with tight clearance on one side
LN2-0S	In-LN2 at cryogenic temperature with open sides
Water-2S	In-water at room temperature with tight clearance on two sides
Water-1S	In-water at room temperature with tight clearance on one side
Water-1S-T*	In-water at room temperature with tighter clearance on one side
LH2-1S	In-LH2 at cryogenic temperature, unpressurized, with tight clearance on one side
LH2-2S-T*	In-LH2 at cryogenic temperature, unpressurized, with tight clearance on one side and tighter clearance on another side

**Note: The average clearance between the plate(s) and the beam for the standard test cases was measured between 0.050 and 0.070 inches. For the tighter clearance cases (Water-1S-T and LH2-2S-T), a smaller washer was used to mount the plate, creating a smaller average gap that was measured between 0.010 and 0.030 inches*

ANSYS modal acoustic models were generated for the tight clearance test configurations shown in Table 1. The same general modeling techniques were used as for the Phase I testing and analysis of the cantilever beam. Due to tight fluid clearances surrounding the beam, fluid volumes were sliced as needed to better control mesh densities throughout the volume. General practice was to ensure at least two elements through the tight fluid clearance. Neither the plates nor the fluid on the side of the plates opposite the cantilever beam were modeled. Addition of this fluid volume could potentially change or improve model results. An example model and finite element mesh showing the tight fluid clearance is shown in Fig. 4.

ANSYS results for the tight clearance water and LH2 cases are shown in Table 2. Given the uncertainty in the actual fluid clearance (as noted in Table 1), the calculated clearance effect compared quite well to test results for the water and LH2 cases. Only the nominal fluid clearances were modeled (i.e. 0.060" and 0.020"). Future modeling could include the bounds of the fluid clearance to analytically predict the natural frequency sensitivity to this clearance. As the purpose of this test and analysis series is to quantify tip clearance effects, the frequency results are

Table 2. Cantilever Beam Test and Analysis Summary

Open Water Configuration					
Mode (Test Order)	Test (Hz)	ANSYS Acoustic FEM (Hz)	% Error		
1	25.25	25.457	0.82%		
2	161.75	160.3	-0.90%		
3	459.75	459.49	-0.06%		
4	911.00	918.34	0.81%		
Water-1S Configuration					
Mode (Test	Test (Hz)	ANSYS Acoustic	% Error	Clearance Effect	
				Test	ANSYS
1	23.25	23.77	2.23%	-7.92%	-6.63%
2	154.25	153.71	-0.35%	-4.64%	-4.11%
3	434.25	436.34	0.48%	-5.55%	-5.04%
4	869.75	886.37	1.91%	-4.53%	-3.48%
Water-2S Configuration					
Mode (Test	Test (Hz)	ANSYS Acoustic	% Error	Clearance Effect	
				Test	ANSYS
1	19.75	20.30	2.78%	-21.78%	-20.26%
2	140.50	132.65	-5.59%	-13.14%	-17.25%
3	398.00	399.83	0.46%	-13.43%	-12.98%
4	832.25	848.66	1.97%	-8.64%	-7.59%
Water-1S-T Configuration					
Mode (Test	Test (Hz)	ANSYS Acoustic	% Error	Clearance Effect	
				Test	ANSYS
1	22.25	22.71	2.05%	-11.88%	-10.81%
2	153.25	143.92	-6.09%	-5.26%	-10.22%
3	427.25	419.33	-1.85%	-7.07%	-8.74%
4	859.75	860.73	0.11%	-5.63%	-6.27%

Open LH2 Configuration					
Mode (Test Order)	Test (Hz)	ANSYS Acoustic FEM (Hz)	% Error		
1	42.50	42.123	-0.89%		
2	267.50	265.37	-0.80%		
3	750.75	747.48	-0.44%		
4	1475.00	1471.5	-0.24%		
LH2-1S Configuration					
Mode (Test Order)	Test (Hz)	ANSYS Acoustic	% Error	Clearance Effect	
				Test	ANSYS
1	42.25	41.77	-1.15%	-0.59%	-0.85%
2	266.25	263.41	-1.07%	-0.47%	-0.74%
3	746.50	743.44	-0.41%	-0.57%	-0.54%
4	1465.50	1467.00	0.10%	-0.64%	-0.31%
LH2-2S-T Configuration					
Mode (Test Order)	Test (Hz)	ANSYS Acoustic	% Error	Clearance Effect	
				Test	ANSYS
1	38.50	39.40	2.34%	-9.41%	-6.46%
2	256.00	250.91	-1.99%	-4.30%	-5.45%
3	726.25	718.42	-1.08%	-3.26%	-3.89%
4	1438.25	1431.20	-0.49%	-2.49%	-2.74%

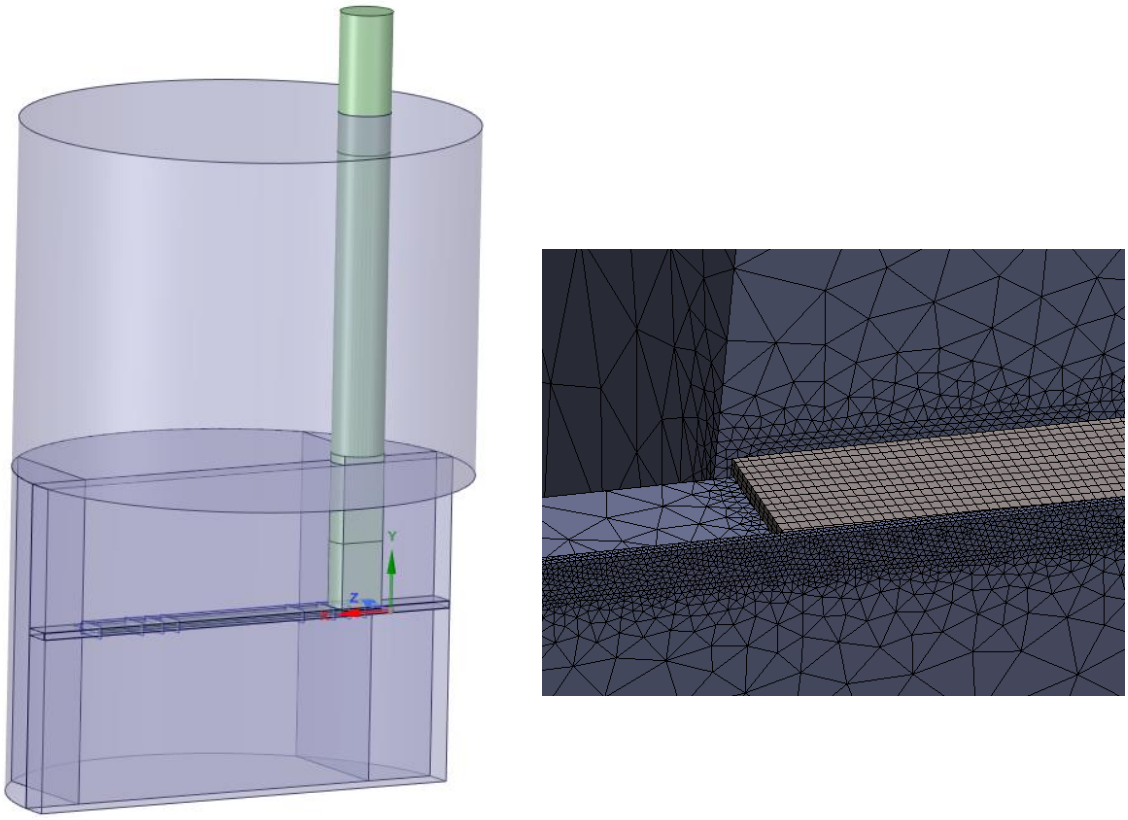

Fig. 4 Cantilever Beam Model for Water-1S Configuration

compared back to the open water (no side-plates) case, focusing on the first cantilever mode since it is most similar to the inducer mode of interest. The results are excellent, with the numerical results matching test generally within 3%.

SUB-SCALE INDUCER MODAL TEST AND ANALYSIS IN AIR AND WATER

The second step in the Phase-II process was to perform a modal test and analytical correlation of the sub-scale inducer in air and a large tub of water. The test was performed in September of 2017, and modes were successfully obtained for the configuration, in which the component was glued to a block to exercise the hub flexibility and the block placed on a foam pad to enable well-defined boundary conditions. A modal punch device was used to apply impact loads to the inducer, and a scanning Laser Doppler Vibrometer (LDV) was used to measure the response, which was then processed to generate natural frequencies and mode shapes. An acrylic strip was placed on the surface of the water to enable a smooth optical transition for the laser beam (see Fig. 5). The blade responses were measured at roughly 0.5" increments along the blade edges as shown in Fig. 5.

Fig. 5 Subscale Inducer Modal Test in Large Tub of Water

Unfortunately, the model correlation proved problematic. After some investigation, it became clear that the inducer exhibited mode localization due to mistuning, a phenomena most commonly observed in turbine bladed-disks in which a nominally cyclic symmetric structure that is in fact not perfectly symmetric due to manufacturing deviations causes substantially warping of the modes shapes (localization) and amplification above the tuned system resonant response. An additional test in air was conducted after removing the strain gages and waterproof tape on the blades (needed for water flow testing) as this was believed to be the source of the mistuning. This test also provided a measurement of how much the blade natural frequencies were affected by the instrumentation. The instrumentation may have increased the mistuning, but localization of the mode shapes was still evident in these "clean" modal air test results. The mistuning is therefore believed to be due to blade geometry variation, which is verified by white light scan results of the inducer showing different surface deviations for each blade compared to the solid model geometry. Localization of the mode shapes made the model correlation difficult. Interestingly, the addition of water does appear to tune the system somewhat, which makes sense as the fluid-added mass is entirely symmetric.

ANSYS modal acoustic models were created for the subscale inducer modal tests in air and water. The mode of interest for the inducer is the second in-phase zero nodal diameter (ND) mode, where the sequential order within this family refers to the number of half-waves along the periphery the blade starting at the leading edge. This is the mode compatible with the HOSC excitation shape [6] and whose natural frequency is in the HOSC excitation

frequency range for the full-scale inducer. The modes of interest found in test were identified by visual inspection and the Modal Assurance Criterion (MAC) was used for verification. The MAC was also used to match the test modes to the ANSYS calculated modes and were verified by visual inspection. Discerning the sequential order of the zero ND mode in test is difficult as several modes in this family look very similar in the portion of the blade visible to the LDV where the responses are measured. For instance, on the blade edge furthest from the leading edge where it meets the adjacent blade, the displacement diminishes, but this can be due to the final half-wave on the blade, or at a nodal line where another half-wave exists on the blade in the non-visual portion.

Two adjustments were made to the analytically calculated frequencies. One was for the effect of fillets since they were not included in the finite element model. This effect was determined by comparing previous modeling including the fillet with fillet-free models, which are substantially more computationally efficient. The second adjustment made was for the effect of the strain gages and waterproof tape. The magnitude of this adjustment was determined from the two air modal tests mentioned above (original test and "clean" test).

The tested modes of interest are shown in Fig. 6 and the analytical mode shapes are shown in Fig. 7. Localization is evident in both air tests indicating that the source of mistuning is not due only to instrumentation. As mentioned above, this localization is diminished in the water test mode shape. A summary of all MAC-matched modes from the air and open-water modal tests are shown in Table 3. The "large volume effect," which is the effect due to fluid added-mass in an open configuration, ranged from approximately -35% to -49%. Table 4 presents the combined test and analysis results for the air and large tub of water cases for the mode of interest. The analytical percent errors to test are less than 5%.

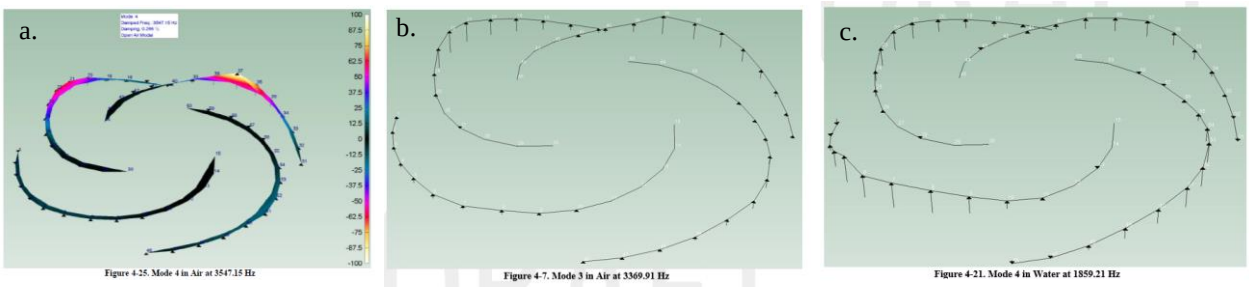

Fig. 6 Subscale Inducer Large Tub Measured Mode Shapes a) Clean Air Test without Strain Gages and Waterproof Tape; b) Air Test with Strain Gages and Waterproof Tape; c) Water Test with Strain Gages and Waterproof Tape

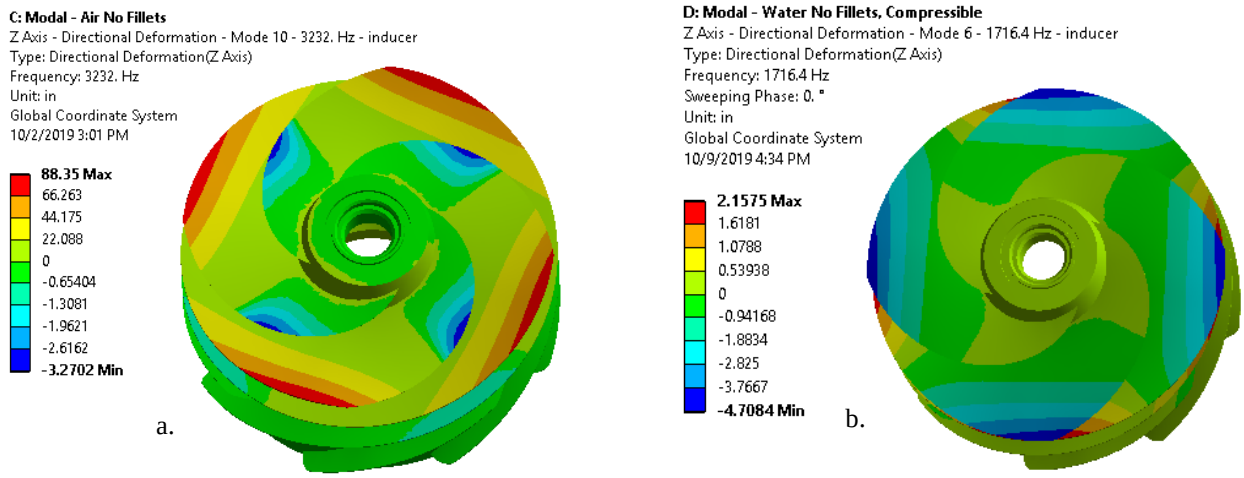

Fig. 7 Subscale Inducer Large Tub Calculated Mode Shapes a) Vacuum b) Compressible Water

Table 3. Subscale Inducer Modal Test Results in Air and Large Volume of Water

Air Test Mode	Modal Test Result Air	Water Test Mode	Modal Test Result Water	Large Volume Effect
	Freq. (Hz)		Freq. (Hz)	(%)
4	3410.06	1	1735.41	-49.11%
2	3301.61	2	1776.34	-46.20%
1	3268.78	3	1783.81	-45.43%
3	3369.91	4	1859.21	-44.83%
8	3723.73	5	2021.63	-45.71%
5	3664.58	6	2146.86	-41.42%
6	3671.73	7	2153.39	-41.35%
7	3701.40	8	2276.46	-38.50%
10	4137.84	9	2474.70	-40.19%
9	4117.99	10	2691.92	-34.63%

SUB-SCALE INDUCER TIGHT TIP-CLEARANCE MODAL TEST AND ANALYSIS IN WATER

In addition to the large water tub test, a tight-tip clearance test was added to the 2018 testing of the sub-scale inducer. A cylinder was machined that provided a 0.035" clearance around the periphery (see Fig. 8), and a modal test was performed using the techniques discussed above. To maintain consistency with the previous large tub modal tests, the tight clearance test was conducted with the strain gages and waterproof tape.

For the mode of interest, the MAC was used to determine modal matches between test and between test and analysis. The tip clearance effect is also shown in Table 4. The ANSYS acoustic finite element model compared well to test data. For the mode of interest the tip clearance effect was calculated to be 15.32% from test and 12.85% from analysis. The test and analytical mode shapes for the tight clearance water test are shown in Fig. 9.

Table 4. Subscale Inducer Test and Analysis Summary for Large Volume of Air and Water

	Test/Model	Fluid	On-blade Instrumentation	Compressibility	Fluid Volume (in)	Radial Clearance from Blade OD (in)	Test or Analytical Freq. (Hz)	Adjusted Analytical Freq. (Hz)	Error to Test (%)	Large Volume Effect (%)	Tip Clearance Effect (%)	Compressibility Effect (%)	Total Reduction from Air (%)
Test	Modal Test	Air	Strain gages and waterproof tape	-	18.75 Diam. Tank	6.38	3369.91						
Test	Modal Test	Air	None	-	18.75 Diam. Tank	6.38	3547.15						
Test	Modal Test	Water	Strain gages and waterproof tape	-	18.75 Diam. Tank	6.38	1859.21						-44.83%
Test	Modal Test	Water	Strain gages and waterproof tape	-	Pipe w/ Avg. Radial Clearance 0.035"	0.035	1574.29				-15.32%		-53.28%
Analysis	Modal Test	Vacuum	-	-	18.75 Diam. Tank	6.38	3232.00	3371.18	-4.96%				
Analysis	Modal Test	Water	-	Incompressible	18.75 Diam. Tank	6.38	1721.90	1796.05		-46.72%			-46.72%
Analysis	Modal Test	Water	-	Compressible	18.75 Diam. Tank	6.38	1716.40	1790.31	-3.71%	-46.72%		-0.32%	-46.89%
Analysis	Modal Test	Water	-	Incompressible	Pipe w/ Avg. Radial Clearance 0.035"	0.035	1500.70	1565.33		-46.72%	-12.85%		-53.57%
Analysis	Modal Test	Water	-	Compressible	Pipe w/ Avg. Radial Clearance 0.035"	0.035	1482.10	1545.93	-1.80%	-46.72%	-12.85%	-1.24%	-54.14%

For reference, a summary of all MAC-matched modes from the large clearance and tight clearance water modal tests are shown below in Table 5. The tip clearance effect varied between approximately -10% to -21%.

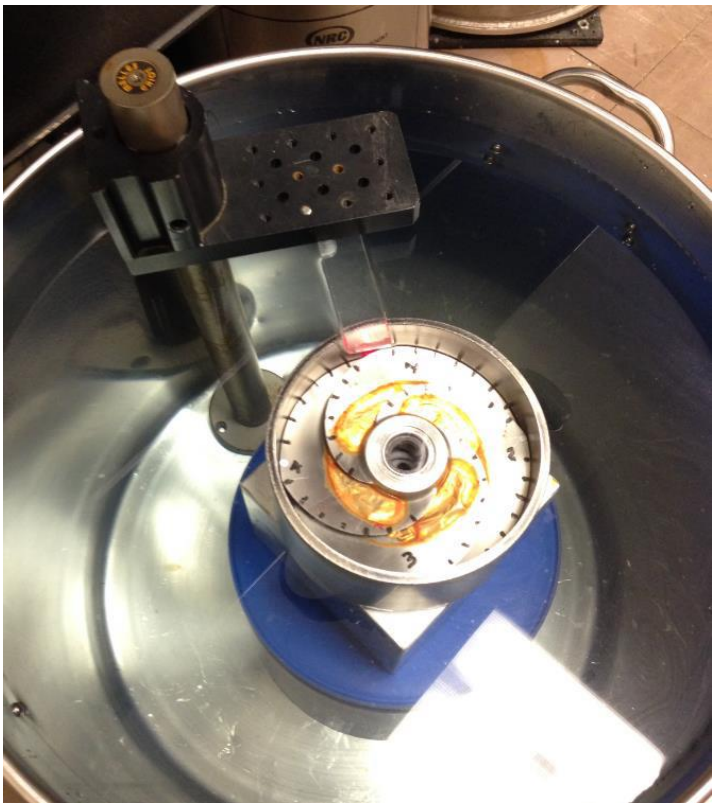

Fig. 8 Subscale Inducer Tight Tip-Clearance Modal Test

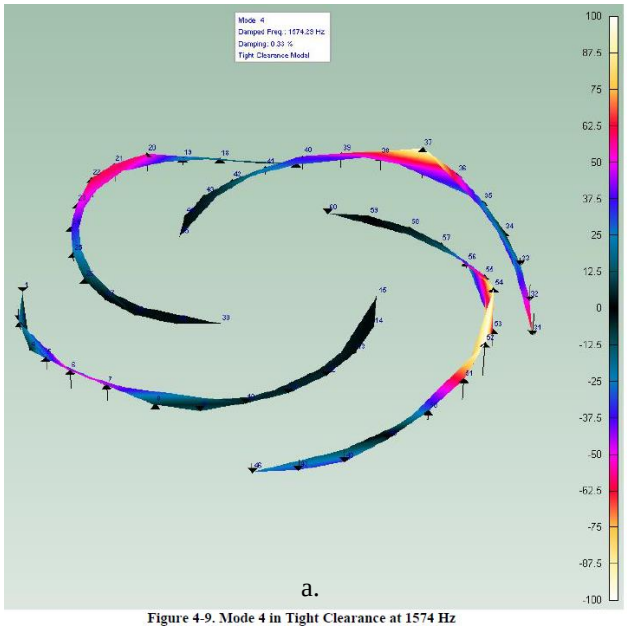

a.

Figure 4-9. Mode 4 in Tight Clearance at 1574 Hz

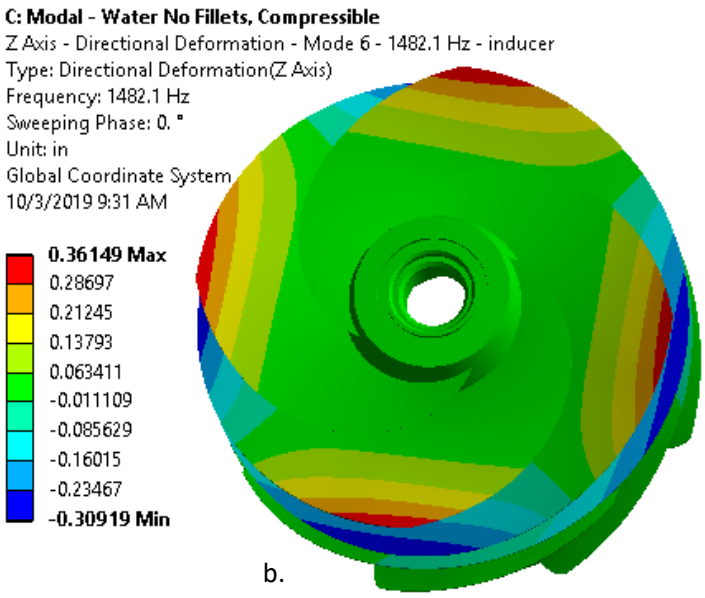

b.

Fig. 9 Subscale Inducer Tight Tip Clearance in Water Mode Shapes a) Test b) Analysis (Compressible Water)

Table 5. Subscale Inducer Modal Test Results in Large and Tight Tip Clearance in Water

Large Volume Water Test Mode	Modal Test Result Large Volume Water	Tight Clearance Water Test Mode	Modal Test Result Tight Clearance Water	Tip Clearance Effect
	Freq. (Hz)		Freq. (Hz)	(%)
1	1735.41	1	1370.43	-21.03%
4	1859.21	4	1574.29	-15.32%
6	2146.86	6	1762.31	-17.91%
7	2153.39	7	1840.63	-14.52%
8	2276.46	8	1945.97	-14.52%
9	2474.7	10	2148.16	-13.20%
10	2691.92	12	2405.18	-10.65%

SUB-SCALE INDUCER PING TEST AND ANALYSIS IN LH2

The final test discussed in this paper is the ping test in the cryogenic test facility. A set of six gages was first mounted to the inducer; this number was limited by the expense of the cryogenic gages and of mounting them, as well as by room necessary for routing the cables out of the cryostat (see Fig. 10). It was believed that by placing three gages on one blade and one gage on each of the other three blades, frequency matches could be determined with modes determined from the previous modal tests. The inducer was then bolted through the center onto a facility "star" piece that would be lowered as an assembly into the cryostat (see Fig. 11). The inducer would then be "plucked" in the same manner as the cantilever beam. As with the cantilever beam testing, a test in air was initially performed to serve as a baseline, followed by the standard test in LH2. A test was then performed with an extra 15 psi of pressurization to qualitatively enable a non-bubbly condition compared to the standard configuration. The LH2 was then allowed to boil off and tests were performed to give cryogenic and several other cold temperature pings without the presence of the fluid. These ping test results were used for calibration of the elastic modulus versus temperature curve of the subscale inducer material. Lastly, a test in liquid Nitrogen was also performed to provide an additional fluid/temperature data point.

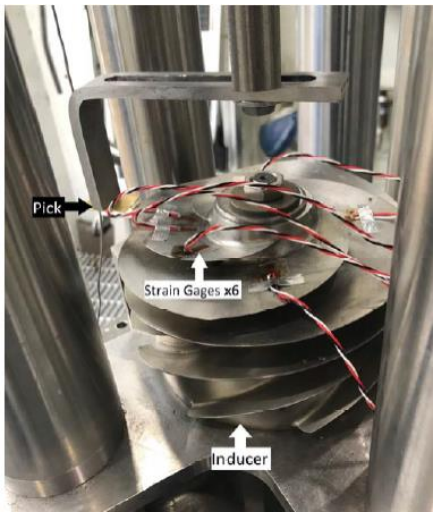

Fig. 10 Subscale Inducer with Strain Gages, Cryostat Mount, and Pick

Fig. 11 Facility Dewar above Cryostat

Strain gage analysis was conducted and modal matches between air and LH2 were made based on the same relative resonant peak location and the same strain gage phasing. Modal matches are shown in Table 6. The mode of interest in air is highlighted in the table. The 3480 Hz frequency measured in LH2 had one blade out-of-phase with the other blades. It is not understood whether this is a product of mistuning, or if perhaps the measured phase of that blade is incorrect. If it was incorrect, this could be a zero nodal diameter mode (the mode of interest). The out-of-phase gage was not the lowest responder and it was not on the blade with two other gages. The estimated cryo air frequency to calculate the reduction from cryo air was based on the cold air ping data when available or the difference between the room temperature and LH2 temperature elastic moduli.

Table 6. Subscale Inducer Ping Test Results in Cryostat, Air and LH2

Mode	Cryostat Test Result Air	Cryostat Test Result Air	Estimated Cryo Air	Cryostat Single Blade Phasing Air			Mode	Cryostat Test Result LH2	Cryostat Test Result LH2	Cryostat Single Blade Phasing LH2			Test Total Reduction from Air	Estimated Reduction from Cryo Air
	Freq. (Hz)	Inducer ND	Freq. (Hz)	Gage1	Gage2	Gage3		Freq. (Hz)	Inducer ND	Gage1	Gage2	Gage3	(%)	(%)
A	3408	2	3497	Out	In	In	A	3204	2	Out	In	In	-5.99%	-8.38%
	3548	0	3638	NA	In	In		3480	?	In	In	In	-1.92%	-4.34%
B	3708	2	3797	NA	In	In	B	3568	2	Out	In	In	-3.78%	-6.03%
C	4132	2	4233	NA	In	In	C	3956	2	NA	In	In	-4.26%	-6.54%
	4240	0		NA	In	In		4292	1	NA	In	In		
E	4592	2	4712	NA	In	In	E	4392	2	In	In	In	-4.36%	-6.79%
D	4632	0	4751	In	In	In	D	4492	0	In	In	In	-3.02%	-5.45%
	4716	1		NA	In	In		4856	2	In	In	In		
	5048	2		NA	In	In		5300	2	In	In	Out		
	5080	1?		NA	In	In		5864	0	In	In	Out		
	5136	0		NA	In	In								
	5488	2		NA	In	NA								
	5964	2		In	In	Out								
	6484	2		In	In	Out								

ANSYS finite element models were constructed for the cryostat air and cryostat LH2 tests (see Fig. 12). The facility star piece and columns were included in the model. The test/analysis correlation procedure used MAC calculations and/or judgement when determining matching modes. In one case the MAC matched modes did not appear to be the

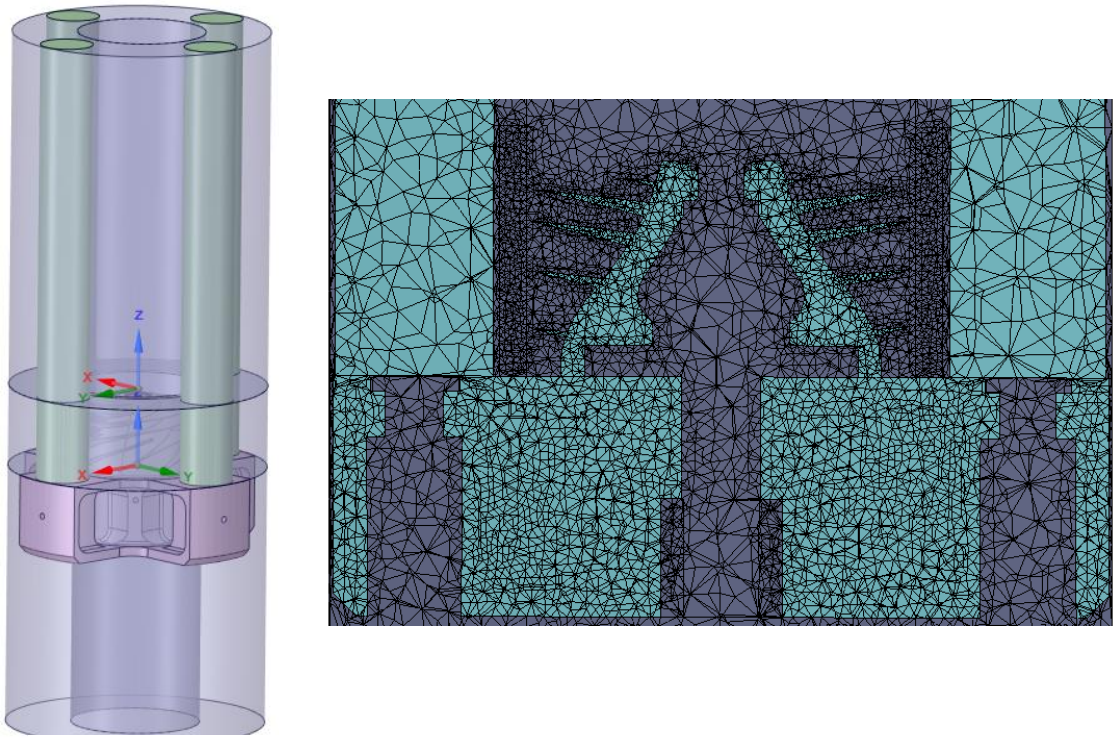

Fig. 12 Solid Model and ANSYS Finite Element Mesh of Subscale Inducer Cryostat LH2 Test

best visual matches and in that case the magnitude of the frequency would not align with test data relationships. In this case the best mode was selected by judgement. The correlation procedure was as follows:

1. *Determine the mode of interest in air in the cryostat*: MAC used to compare clean modal test in air mode shape to ANSYS modal acoustic mode shapes for cryostat air test. The analytical mode selected was verified to agree with measured strain gage phasing in air in the cryostat.
2. *Select the analytical mode of interest in incompressible LH2*: MAC used to compare ANSYS cryostat air mode shapes to ANSYS cryostat incompressible LH2 mode shapes. The closest MAC-matched LH2 mode was not the best visual match. It would also result in a total reduction from air that would be out of family with test data. An alternate match was made.
3. *Select analytical mode of interest in compressible LH2*: MAC used to compare ANSYS cryostat incompressible LH2 mode shapes to ANSYS cryostat compressible LH2 mode shapes. The closest compressible match was selected.
4. *Compare ANSYS cryostat compressible LH2 mode of interest to measured modes in LH2 cryostat test (compare frequency and strain gage phase information)*: The measured mode of interest in LH2 was originally believed to be 3480 Hz. However, the phase information is not understood and the total reduction from air and estimated reduction from cryo air appears out of family with other matched modes. This is not yet understood.

The analytical modes of interest in the cryostat are shown in Fig. 13. The combined test and analysis results are shown below in Table 7.

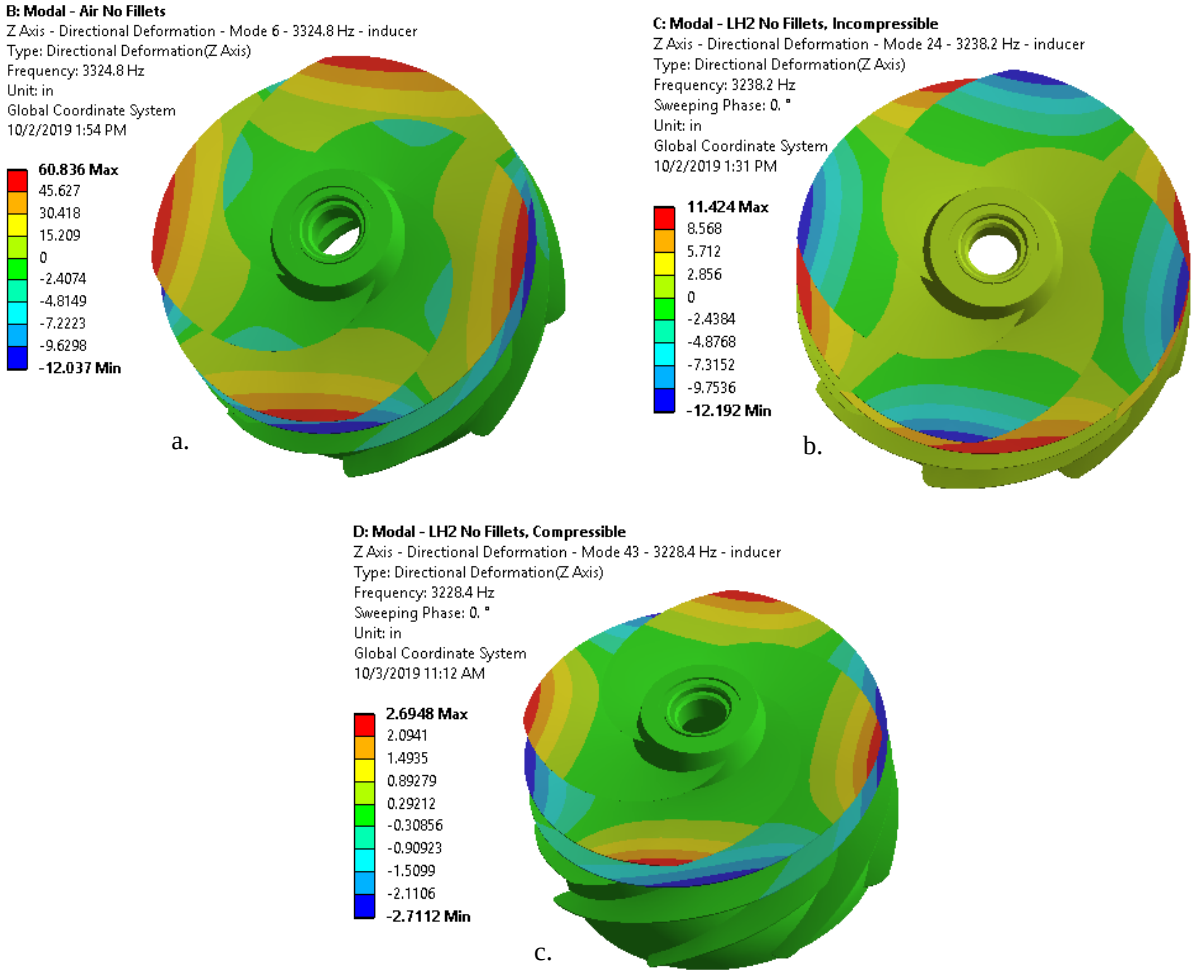

Fig. 13 Subscale Inducer Cryostat Analytical Modes of Interest a) Air b) Incompressible LH2 c) Compressible LH2

Table 7. Subscale Inducer Test and Analysis Summary for Air and LH2

	Test/Model	Fluid	On-blade Instrumentation	Compressibility	Fluid Volume (in)	Radial Clearance from Blade OD (in)	Test or Analytical Freq. (Hz)	Adjusted Analytical Freq. (Hz)	Error to Test (%)	Modulus Effect (%)	*Large Volume Effect (%)	Compressibility Effect (%)	Total Reduction from Air (%)
Test	Cryostat	Air	Cryo gages	-	12.875 Diam. Cryostat, with 4 columns	3.44 (Cryostat), 0.74 to columns	3548.00						
Test	Cryostat	LH2	Cryo gages	-	12.875 Diam. Cryostat, with 4 columns	3.44 (Cryostat), 0.74 to columns	3480.00						-1.92%
Analysis	Cryostat	Vacuum	-	Incompressible	12.875 Diam. Cryostat, with 4 columns	3.44 (Cryostat), 0.74 to columns	3324.80	3467.98	-2.26%				
Analysis	Cryostat	Cryo Vacuum	-	Incompressible	12.875 Diam. Cryostat, with 4 columns	3.44 (Cryostat), 0.74 to columns	3407.92	3554.68		2.50%			
Analysis	Cryostat	LH2	-	Incompressible	12.875 Diam. Cryostat, with 4 columns	3.44 (Cryostat), 0.74 to columns	3238.20	3377.65		2.50%	-4.98%		-2.60%
Analysis	Cryostat	LH2	-	Compressible	12.875 Diam. Cryostat, with 4 columns	3.44 (Cryostat), 0.74 to columns	3228.40	3367.43	-3.23%	2.50%	-4.98%	-0.30%	-2.90%

An important item to note regarding the table above is the calculation of the "large volume effect". A comparative analysis was run without the columns in the cryostat (the elements were converted to fluid). When this was done the frequency of interest increased by 1.63%. However, in the analytical model the columns were aligned with the inducer blade leading edge tip, which may not have been their position in test. Further frequency increase could also occur with a fluid volume greater than 3.44" radial clearance from the inducer blade. In summary, the calculated large volume effect may include some tip clearance effect. Additional analytical work could quantify this.

COMBINED RESULTS & EXTRAPOLATION OF TECHNIQUES TO SLS FULL-SCALE INDUCER

The ultimate goal of this integrated test and analysis program is to ease or eliminate restrictions on the full-scale RS-25 Low Pressure Fuel Pump (LPFP) inducer. MSFC has pursued numerous parallel paths to this goal involving inducer damping, the HOSC forcing function and the natural frequency uncertainty. The test data and calibrated analytical models presented in this paper are intended to reduce the natural frequency uncertainty, and perhaps refine the predicted natural frequency of interest such that the resonant crossing with HOSC is eliminated. In order to use these analytical methods on the full-scale inducer, success must be demonstrated in the ability to model structures in LH2 and structures with tight fluid clearances. The authors believe that sufficient success has been shown to extend these techniques to the full-scale inducer (as presented above). Future analysis of uncertainty could incorporate calculated analytical errors to test.

SSME LPFP full-scale inducer modal test data in air and water were used for initial ANSYS modal acoustic model calibration. From that point, analyses were completed to track natural frequency due to following effects: Temperature/elastic modulus change, presence of large LH2 fluid volume, tip clearance effect, and compressibility effects (Table 6). After identifying the analytical mode of interest in vacuum, the MAC was used to compare each subsequent result back to the vacuum air mode shape.

The natural frequency reduction in a large tank of water is -58%. The reduction due to a large volume of LH2 was calculated to be almost -13% (excluding elastic modulus effect). The analytical trend of results for tip clearance effect are not yet understood as that effect is expected to increase with decreased clearance. The average tip clearance effect is -11% for the range of tip clearances analyzed. The compressibility effect was calculated, but more work is needed to better understand the interaction of the structural and acoustics modes and the associated magnitude of the effect, especially since an acoustics analysis with the inducer as a rigid structure identified acoustic modes near the structural modes. In addition, it was found that this effect varied depending on the tip clearance. Two results are listed for the compressible case of a large volume of LH2. The MAC identified both as similarly good matches, thus both have been reported.

For the RS-25 full-scale inducer the tip clearance effect was originally estimated to be substantially less than the values calculated per Table 6. Given the magnitude of this effect measured for the MSFC cantilever beam, RS-25 subscale inducer, and as reported by Xiu and Davis [4], the authors believe that this effect is substantial for the RS-25 full-scale inducer as shown in Table 8. This effect further decreases the natural frequency of interest and that decrease may be sufficient to clear the resonance for SLS and thus remove the inducer hardware restrictions.

Table 8. Full Scale Inducer Test and Analysis Summary for Air, Water and LH2

	Boundary Condition	Fluid	Temperature	Compressibility	Fluid Volume (in)	Radial Clearance from Blade OD (in)	Error to Test (%)	Modulus Effect (%)	Large Volume Effect (%)	Tip Clearance Effect (%)	Compressibility Effect (%)	Total Reduction from Air (%)
Test	Free and In-Situ (6)	Air	RT	Incompressible	Large							
Test	Free (3)	Water	RT	Incompressible	Large				-57.5%			-57.5%
Analysis	Free	Vacuum	RT	Incompressible	Large		1.9%					
Analysis	Free	Water	RT	Incompressible	Large	13.5	0.2%		-58.2%			-58.2%
Analysis	Free	Vacuum	Cryo	Incompressible	Large			4.6%				
Analysis	Free	LH2	Cryo	Incompressible	Large	13.5		4.6%	-12.8%			-8.9%
Analysis	Free	LH2	Cryo	Compressible	Large	13.5		4.6%	-12.8%		-4.2%	-12.7%
Analysis	Free	LH2	Cryo	Compressible	Large	13.5		4.6%	-12.8%		-0.9%	-9.7%
Analysis	Free	LH2	Cryo	Incompressible	Tight	0.005		4.6%	-12.8%	-11.1%		-19.0%
Analysis	Free	LH2	Cryo	Compressible	Tight	0.005		4.6%	-12.8%	-11.1%	-4.1%	-22.4%
Analysis	Free	LH2	Cryo	Incompressible	Tight	0.0015		4.6%	-12.8%	-13.2%		-20.9%
Analysis	Cryo	LH2	Cryo	Compressible	Tight	0.0015		4.6%	-12.8%	-13.2%	2.5%	-18.9%
Analysis	Free	LH2	Cryo	Incompressible	Tight	0.0035		4.6%	-12.8%	-9.2%		-17.9%
Analysis	Free	LH2	Cryo	Compressible	Tight	0.0035		4.6%	-12.8%	-9.2%	-9.7%	-25.9%

CONCLUSIONS & FUTURE WORK

An integrated test and analysis program was developed at NASA/MSFC to mitigate the restrictions of the RS-25 LPFP inducer due to potential resonance excitation with HOSC. The first phase of this program was completed in 2017 and reported by the authors. Phase I included the detailed testing and analytical calibration of a titanium cantilever beam in large volumes of water and LH2. The calibrated analysis techniques using ANSYS modal acoustics were very accurate with percent errors less than 1% for the first four cantilever beam modes in both liquids. The second phase of this program reported here included tip clearance testing of the cantilever beam in water and LH2, as well as modal and ping testing of a subscale RS-25 LPFP inducer in air, water, and LH2.

The tip clearance effects measured for cantilever beam and inducer are substantial and cannot be neglected in the estimation of natural frequency. For the cantilever beam, several different tight tip clearance configurations were tested. The beam first natural frequency reduced as much as 20% in water and 9% in LH2 when there was a tight clearance on both sides of the beam. Given there was uncertainty in the actual clearance (due to difficulty in measuring this clearance in the cryostat), the ANSYS results generally matched the test quite well. The largest error to test was around 3% for the LH2 2S-T configuration.

A tight tip clearance modal test in water was completed for the RS-25 LPFP subscale inducer. As for the cantilever beam, the measured tip clearance effect was substantial. The natural frequency of the mode of interest reduced by 15% and the reduction was as high as 21% for other modes. The calibrated ANSYS model predicted the tip clearance effect to within 2.5% of the test results.

Ping testing of the subscale inducer was completed in LH2. Measured modes in air and LH2 were matched to determine the total reduction from air and the reduction from cryo air (also called the large volume effect). While there is uncertainty as to whether the mode of interest was found in the LH2 test, the analytical results for the large volume effect match well with the effect measured for the other modes. Analysis predicts a natural frequency reduction of 5% due to the presence of a large volume of LH2 (excluding elastic modulus effects). For all measured modes, this reduction varied roughly between 5% and 8%. A third phase of inducer testing with a tight tip clearance in LH2 is being considered to further validate analytical capability to predict the tip clearance effect for the inducer.

Finally, these calibrated ANSYS modal acoustic techniques were extended to the SLS RS-25 LPFP full-scale inducer. Effects due to elastic modulus, large volume, tip clearance, and compressibility were tracked separately. The refinement of these adjustments may help to mitigate the inducer HOSC resonance concerns for SLS. The demonstrated success to model structures in LH2 with tight clearances will benefit future flight programs as well.

REFERENCES

[1] Brown, Andrew M., DeLessio, Jennifer L., Jacobs, Preston W., "Natural Frequency Testing and Model Correlation of Rocket Engine Structures in Liquid Hydrogen – Phase I, Cantilever Beam," Proceedings of the 36th IMAC, A Conference and Exposition on Structural Dynamics, Orlando, Florida, Feb. 12-15, 2018.

[2] Harrison, C., Tavernier, E., Vancauwenberghe, O., Donzier, E., Hsu, K., Goodwin, A. R. H., Marty, F., Mercier, B., "On the response of a resonating plate in a liquid near a solid wall," Sensors and Actuators A 134 (2007) 414-414.

[3] Sader, John E., "Frequency response of cantilever beams immersed in viscous fluids with applications to the atomic force microscope," Journal of Applied Physics, Vol. 84, No. 1, 1 July 1998, pp. 64-76

[4] Xiu, H., Davis, R. Benjamin, Romeo, Ryan C., "Edge clearance effects on the added mass and damping of beams submerged in viscous fluids," Journal of Fluids and Structures 83 (2018) 194-217.

[5] Davis, R. Benjamin, Virgin, Lawrence N., Brown, Andrew M., "Cylindrical Shell Submerged in Bounded Acoustic Media: A Modal Approach," AIAA Journal, Vol. 46, No. 3, pp. 752-763.

[6] Subbaraman, Maria, Burton, Kevin, "Cavitation-Induced Vibrations in Turbomachinery: Water Model Exploration," Fifth International Symposium on Cavitation, Osaka, Japan, November 1-4, 2003